formation of the I-arene complex from I_2 and the $[Ar^{+}\cdot,I_2^{-}\cdot]$ lifetime is greater than ~10 ps, the absorption spectra of $I^{2-}\cdot$ and $AR^{+}\cdot$, in principle, should appear in the time-resolved absorption spectra in the wavelength range of ~350-835 nm. For 532-nm excitation of I_2-BEN, I_2-TOL, or I_2-MES solutions, no absorption bands besides the tailing absorption of the I-arene complex were observed in the 630-nm to 835-nm region at times ranging from -8 to ~50 ps after excitation.

In regard to the presence of $I_2^{-}\cdot$, this radical anion has been reported to exhibit an absorption maximum at ~370 nm.[16] For those measurements,[16] $I_2^{-}\cdot$ was generated by means of microsecond-pulsed excitation of aqueous I^-, presumably via

$$I^- \xrightarrow{h\nu} I\cdot + e^-$$

$$I\cdot + I^- \rightarrow I_2^{-}\cdot$$

However, electron attachment to I_2 is dissociative, proceeding via the $^2\prod$ g repulsive state to give I^- and $I\cdot$.[17] This dissociative electron attachment is akin to the process that would give rise to $I_2^{-}\cdot$ via CT excitation of an I_2-arene complex. Therefore, $I_2^{-}\cdot$ generated in this manner probably has a lifetime of < 10 ps and would not be detected in our experiment. Indeed, interrogation of I_2-TOL and I_2-MES in the 360-nm to 395-nm region, after sample excitation at 532-nm, provides no evidence for the existence of a transient absorption at ~370 nm that could be assigned to $I_2^{-}\cdot$.

Although we cannot detect the presence of $I_2^{-}\cdot$, we assign the early time-dependent absorbance changes in the transient absorption spectra to the rapid formation and decay of the respective arene cation radical. $BEN^{+}\cdot$, $TOL^{+}\cdot$, and $MES^{+}\cdot$ are expected to exhibit absorption bands in the region of 400-500 nm. From the photodissociation spectra of several methyl-substituted benzene ions, the visible absorption bands of $TOL^{+}\cdot$, $MES^{+}\cdot$, and $HMB^{+}\cdot$ (hexamethylbenzene cation radical) in the gas phase exhibit maxima at 416, 456, and 463, respectively.[18] Of course, shifts of γ_{max} are expected from the gas phase to solution. A basis for comparison of gas-phase and solution absorption spectra is provided by the $HMB^{+}\cdot$ absorption spectrum with $\lambda_{max} \cong 495$ nm in acetonitrile[19] vs. $\lambda_{max} = 463$ nm in the gas phase nm in the gas phase. Also, $TOL^{+}\cdot$ exhibits an absorption maximum at 430 nm in a frozen argon matrix.[20] From these observations, we expect absorption maxima in solution at wavelengths that are ~20-30 nm longer than those given in ref 18 that are based upon photodissociation spectra.

In the time-resolved spectra presented in Figures 1-5, the absorption spectrum of $AR^{+}\cdot$ also is superimposed upon the two time-dependent absorption spectra described previously, namely the bleach of ground-state I_2 absorption and the positive absorbance change corresponding to the formation of the I-AR complexes. These superpositions make a quantitative and qualitative evaluation of the reaction mechanism outlined in Scheme I difficult. The I_2-MES samples provides the greatest separation among absorptions of $AR^{+}\cdot$, ground-state I_2, and I-MES complex for the series of solvents studied here. For excitation at either 355 or 532 nm, there is evidence for the presence of $AR^{+}\cdot$ and, therefore, for $[AR^{+}\cdot,I_2^{-}\cdot]$ as an extremely short-lived species.

In summary, our results indicate that photodissociation of I_2 in arene solution is affected to a certain extent by the fact that I_2 is weakly bound to an arene molecule. There is also evidence for the existence of the radical-ion pair $[AR^{+}\cdot,I_2^{-}\cdot]$ with a lifetime of < 10 ps but no experimental evidence of a cage effect involving recombination of two I atoms. We also observe that identical time-dependent absorbance changes occur at times less than ~4 ns for excitation of I_2 solutions in BEN, TOL, and MES regardless of excitation wavelength. Specifically excitation either at 355 nm, a wavelength within the CT absorption band of the I_2-AR complex, or at 532 nm, a wavelength associated with absorption of light by the I_2 molecule, which is bound, to a significant extent, to an arene molecule generates the same species.

(20) Andrews, L.; Keelan, B. W. *J. Am. Chem. Soc.* **1980**, *102*, 5732.

Comparison of Gas-Phase and Electrochemical Hydrogenation of Ethylene at Platinum Surfaces

Andrzej Wieckowski,[†] Stephen D. Rosasco,[†] Ghaleb N. Salaita,*[†,§] Arthur Hubbard,[†] Brian E. Bent,[‡] Francisco Zaera,[‡,⊥] David Godbey,[‡] and Gabor A. Somorjai[‡]

Contribution from the Department of Chemistry, University of California, Santa Barbara, California 93106, and The Materials and Molecular Research Division, Lawrence Berkeley Laboratory, Department of Chemistry, University of California, Berkeley, California 94720.
Received November 30, 1984

Abstract: Rates of hydrogenation of ethylene to ethane under gas-solid (G-S) and liquid-solid (L-S) (i.e., electrochemical) conditions at well-defined Pt(111) and smooth polycrystalline Pt surfaces are compared. The activation energies are 5.9 kcal/mol for the L-S reaction and 10.8 kcal/mol for the G-S reaction. Comparison of the rate laws under appropriate conditions shows that the hydrogenation proceeds by different reaction mechanisms at the two different interfaces. We have used surface science techniques (low-energy electron diffraction, Auger electron spectroscopy, high-resolution electron energy loss spectroscopy, temperature-programmed desorption) and electrochemistry (a combination of solution and ultrahigh vacuum procedures) to characterize the adsorbed species formed under G-S and L-S reaction conditions and gain insight into the reaction mechanisms. We propose that in hydrogenation at the L-S interface, ethylene is reduced on the Pt surface by adsorbed H atoms, while during hydrogenation at the G-S interface, H atoms must be transferred from the Pt surface through a layer of irreversibly adsorbed ethylene to ethylene that is adsorbed on top of this layer.

One of the fundamental questions of surface chemistry is how chemical changes that occur at gas-solid (G-S) interfaces compare with those at the liquid-solid (L-S) interface. These two heterogeneous processes are intrinsically similar—both involve mass transfer to and from the surface, adsorption, desorption, and chemical reactions at the surface (Figure 1). However, the molecular structures and chemical reactions in the interfacial regions are possibly quite different due to the effects of higher molecular flux, solvent, and electrode potential at the L-S interface. Consequently, atomic surface structure, adsorption, and

§ Fullbright Scholar. Permanent address: University of Jordan, Amman, Jordan.
⊥ Present Address: Brookhaven National Laboratory, NSLS Department, Upton, NY 11973.
† University of California, Santa Barbara.
‡ University of California, Berkeley.

0002-7863/85/1507-5910$01.50/0

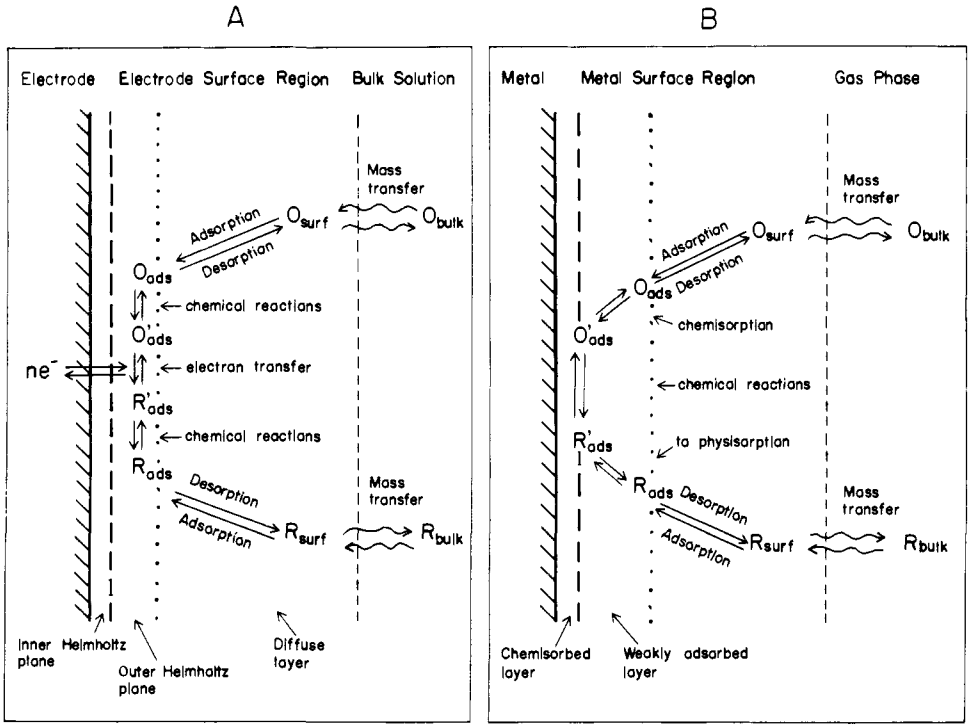

Figure 1. Intrinsic similarities between electrochemical reduction at a metal electrode in solution (A) and reaction of gas-phase molecules at a metal surface (B). The presence of solvent molecules and the effect of the electrode potential in electroreductions are the main differences between these two processes.

chemical rearrangements should all be investigated at G–S and L–S interfaces on the same surface and using the same adsorbate or reactant molecules under similar experimental conditions to establish correlations between the reaction mechanisms at these interfaces.

There are a few catalytic reactions that occur under very similar experimental conditions at the G–S and L–S interfaces. Ethylene hydrogenation to ethane is one of them. This facile reaction readily occurs on platinum and other transition-metal surfaces in both gas and solution phases at 300 K (G–S,[1-4] L–S[5-12]). There are further similarities between ethylene hydrogenation in these two phases. Recent work shows that at both G–S and L–S interfaces the hydrogenation rate is not sensitive to the crystallographic orientation of the Pt surface.[4,5] Studies of deuterium scrambling in L–S ethylene hydrogenation over polycrystalline Pt surfaces[6] show a deuterium distribution similar to that found for hydrogenations at the G–S interface over Pt(111) crystal faces:[4] the product distribution of deuterium displays maximum yield at 1–2 deuteriums per ethane, although products all the way to C_2D_6 are observed. The rate of ethylene H–D exchange in both cases is estimated to be 10–20% of that for hydrogenation.

This reaction, then, appears to be an excellent choice to explore the similarities and differences of the kinetics and mechanisms at the G–S and L–S interfaces, and platinum is a good choice to serve as a catalyst.

In this paper we compare the results of our studies[4,5] of ethylene hydrogenation over single-crystal and annealed, polycrystalline platinum surfaces at the G–S and L–S interfaces at 300 K. New data are presented on the structure and reactivity of chemisorbed ethylene at both interfaces. As far as we know, this is the first attempt to compare catalytic reactions at these two interfaces.

Our data on the structure and reactivity of chemisorbed ethylene under ethylene hydrogenation reaction conditions at the G–S and L–S interfaces were obtained over single-crystal Pt surfaces. Surface science techniques [Auger electron spectroscopy (AES), low-energy electron diffraction (LEED), temperature-programmed desorption (TPD), and high-resolution electron energy loss spectroscopy (HREELS)] were utilized in ultrahigh vacuum (UHV) to characterize adsorbed species before and after reactions in microreactors that were constructed in combination with the UHV chambers. Electrochemical techniques (cyclic voltammetry and chronoamperometry) and a ^{14}C radiotracer technique were used to characterize the reactivity of the adsorbed species.

Our results show that the structure and reactivity of ethylene chemisorbed on Pt is different under G–S and L–S conditions. As a result, the L–S and G–S hydrogenation processes occur via different pathways. Ethylene in the L–S hydrogenation is reduced directly on the Pt surface by adsorbed H atoms. In the G–S hydrogenation, hydrogen atoms must be transferred from the surface to ethylene that is adsorbed on top of a layer of irreversibly adsorbed hydrocarbon fragments. The activation energy for the L–S hydrogenation is substantially lower than that for the G–S hydrogenation 5.9 vs. 10.8 kcal/mol). TPD results in ultrahigh vacuum for the G–S hydrogenation of C_2H_4 over a deuterium-covered surface support the fact that the lower activation energy for the L–S hydrogenation is related to a process where ethylene is adsorbed directly on a hydrogen-saturated platinum metal surface. On the basis of the experimental evidence, we have proposed molecular models for the different reaction mechanisms that occur at the two interfaces.

Experimental Section

We briefly describe here the techniques and procedures used to study the structure and reactivity of chemisorbed ethylene. The UHV cham-

(1) Rylander, P. N. "Catalytic Hydrogenation over Pt Metals"; Academic Press: New York, 1967.
(2) Horiuti, J.; Miyahara, K. *Natl. Stand. Ref. Data Ser. (U.S., Natl. Bur. Stand.)* **1968**, *NSRDS-NBS 13*.
(3) Thomson, S. J.; Webb, G. *J. Chem. Soc., Chem. Commun.* (**1976**), *526*, and references therein.
(4) Zaera, F.; Somorjai, G. A. *J. Am. Chem. Soc.* **1984**, *106*, 2288.
(5) Hubbard, A. T.; Young, M. A.; Schoeffel, J. A. *J. Electroanal. Chem.* **1980**, *114*, 273 and references therein.
(6) Langer, S. H.; Feiz, I.; Quinn, C. P. *J. Am. Chem. Soc.* **1971**, *93*, 1092.
(7) Fukikawa, K.; Kita, H. *J. Chem. Soc., Faraday Trans. 1* **1979**, *75*, 1638.
(8) Kita, H. *Isr. J. Chem.* **1979**, *18*, 152.
(9) Triaca, W. E.; Rabockai, T.; Arvia, A. J. *J. Electrochem. Soc.* **1979**, *126*, 218.
(10) Furuya, N.; Motoo, S. *J. Electroanal. Chem.* **1979**, *100*, 771.
(11) Fujikawa, K.; Kita, H.; Sato, S. *J. Chem. Soc., Faraday Trans. 1* **1981**, 3055.
(12) Masue, T.; Kita, H. *Denki Kagaku oyoki Kogyo Butsuri Kagaku Kagaku* **1983**, *51*, 250.

Table I. Kinetic Parameters for L–S Hydrogenation of Ethylene on an Annealed Polycrystalline Pt Electrode

	H-covered Pt[a]	C_2H_4-pretreated Pt[b]	chemisorbed C_2H_4[c]
activation energy, kcal/mol[d]	5.9	6.6	3.3
kinetic isotope effect, k_H/k_D	2.0	2.2	1.2
reaction rate, (molec/Pt surface atom)/s[e]	108	33	1.6
reaction order (C_2H_4)[f]	0	0	
pH dependence, d(log rate)/dpH	−1	−1	
Tafel slope, dE/d(log rate), mV[g]	40	40	107

[a] C_2H_4 in contact with a clean Pt surface at −0.200 V vs. AgCl/Ag reference, $[H^+]$ = 1 M. [b] Chemisorption of C_2H_4 at +0.200 V; reduction of ethylene from bulk solution at −0.200 V, $[H^+]$ = 1 M. [c] Chemisorption of C_2H_4 at +0.200 V; reduction in ethylene-free electrolyte at −0.200 V, $[H^+]$ = 1 M. [d] Temperature was varied from 0 to 50 °C. [e] Temperature = 298 K. To convert these rates to currents (A), multiply by 2.1×10^{-4}. [f] Pressure was varied from 10 to 760 torr (from 4×10^{-5} to 3×10^{-4} M); all L–S data refer to 760 torr. [g] Potential region, −0.100 to −0.200 V vs. AgCl/Ag reference.

ber/reactor systems for G–S[4,13–15,43] and L–S[16–18] reaction studies have been described. With several surface science techniques (AES, TPD, LEED, and HREELS) in the UHV chambers, we characterize the clean or adsorbate-covered Pt surfaces before and after reaction in solution or at atmospheric gas pressures. The Pt(111) single-crystal surfaces were cut and mounted to minimize the amount of polycrystalline Pt.[4,16–18] G–S and L–S adsorbate characterization procedures are described below.

Reactions of the G–S chemisorbed ethylene are carried out by isolating the Pt single crystal in a "high pressure" cell after cleaning in vacuum.[4] Surface structure and composition are analyzed upon return of the crystal to UHV by TPD, HREELS, and a ^{14}C radiotracer technique. In the present comparison, previous results of these techniques are summarized, and new HREELS and TPD data are presented on the coadsorption and reaction of $H_2(D_2)$ with adsorbed C_2H_4. TPD was used to determine desorption products and activation energies. HREEL spectroscopy (reviewed, ref 21) was used to get a vibrational "fingerprint" of the surface structure. HREEL spectra before and after treatment of chemisorbed ethylene with 1 atm of H_2/D_2 were used to confirm adsorbate structure and stability.

In the L–S studies the well-defined Pt(111) clean surface, or the surface pretreated with G–S adsorbed ethylene, was positioned in the electrochemical cell compartment, valved off from the LEED chamber, and brought to atmospheric pressure with argon. Solution was introduced into the cell and electrochemical characterization carried out by using conventional potentiostatic circuitry and procedures.[22] After electrolysis, the liquid was drained, and after brief sorption, cryogenic, ionization, and getter pumping, the crystal was characterized by LEED, AES, and TPD.

Electrochemistry using thin-layer cells has been reviewed.[23,24] The thin-layer electrode (TLE) employed for this study was described in ref 25. An annealed, polycrystalline Pt electrode in a semiinfinite system was used for kinetic study under chronoamperometric[26] conditions.

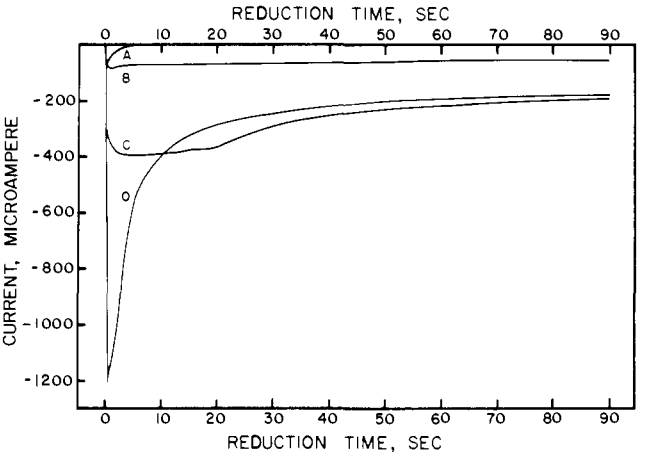

Figure 2. Chronoamperometric current–time curves for reduction of ethylene at an annealed polycrystalline platinum electrode at −0.15 V. (A) Reduction of L–S chemisorbed ethylene; (B) reduction of ethylene from solution at an I-pretreated surface; (C) reduction of ethylene at a Pt surface pretreated with ethylene at 0.2 V; (D) reduction of ethylene at an H-covered surface.

$HClO_4$ solution, 1 M, was used in the L–S study as supporting electrolyte and nitrogen (Linde, oxygen-free grade) as inert gas. If not otherwise stated, the concentration of ethylene in the supporting electrolyte was 4×10^{-3} M. Potentials are reported with respect to AgCl/Ag half-cell prepared with 1 M NaCl. Reagents used in both the G–S and L–S studies were the same as in previous work (ref 4 for G–S and ref 5 for L–S). The concentration of ethylene was varied in the L–S reactions by passing a mixture of ethylene and nitrogen through the solution.

Results and Discussion

1. Rates and Kinetic Parameters. Throughout this comparison of G–S and L–S hydrogenations, we will address the question of how best to compare gas-phase and solution reaction data. We already noted the qualitative similarities of these two heterogeneous processes in the introduction (Figure 1). In this section we first present and discuss some new results on the rates and kinetic parameters of L–S hydrogenation of ethylene. Next we compare the rate laws for L–S and G–S hydrogenation processes over the Pt surfaces.

L–S ethylene hydrogenation kinetic parameters can be extracted from chronoamperometric (current vs. time) data.[26] Such data obtained at −0.15 V are shown for contrasting cases in Figure 2 and Table I: reduction of chemisorbed ethylene, Figure 2A; reduction of ethylene from solution at an I-pretreated surface, Figure 2B; reduction of ethylene at a Pt surface pretreated with ethylene at 0.2 V, Figure 2C; reduction of ethylene at an H-covered surface, Figure 2D. From Figure 2D we see that L–S ethylene reduction occurs 3-fold more rapidly on a surface that has not had opportunity to acquire a layer of adsorbed hydrocarbon (of the type which forms spontaneously at open circuit or at 0.2 V, Figure 2C). Comparison of Figure 2 part B with part D reveals that a layer of chemisorbed I atoms decreases the rate of reduction more than 10-fold relative to the clean Pt surface. This is as expected because the iodine atomic layer prevents adsorption of ethylene and greatly attenuates the amount of adsorbed hydrogen.[5] Ethylene acts as a blocking agent toward its own reduction but adsorbed iodine blocks (although not completely) the reaction even more severely.

Referring to Table I, the kinetic isotope effect of D_2O on L–S reduction of ethylene from the bulk solution is relatively large (K_H/K_D = 2–2.2) compared with that for the chemisorbed layer (K_H/K_D = 1.3). Large isotopic dependences are indicative of mechanisms involving breakage or formation of a specific H–X bond in the rate-determining step.[27] (Previous electrochemical examples of this phenomenon have been discussed in ref 28.)

(13) Blakely, D. W.; Kozak, E.; Sexton, B. A.; Somorjai, G. A. *J. Vac. Sci. Technol.* **1976**, *13*, 1901.
(14) Gillespie, W. D.; Herz, R. K.; Peterson, E. E.; Somorjai, G. A. *J. Catal.* **1981**, *70*, 147.
(15) Davis, S. M.; Zaera, F.; Somorjai, G. A. *J. Am. Chem. Soc.* **1982**, *104*, 7453.
(16) Hubbard, A. T.; Stickney, J. L.; Rosasco, S. D.; Soriaga, M. P.; Song, D. *J. Electroanal. Chem.* **1983**, *150*, 165.
(17) Stickney, J. L.; Rosasco, S. D.; Song, D.; Soriaga, M. P.; Hubbard, A. T. *Surf. Sci.* **1983**, *130*, 326.
(18) Wieckowski, A.; Rosasco, S. D.; Schardt, B. C.; Stickney, J. L.; Hubbard, A. T. *Inorg. Chem.* **1984**, *23*, 565.
(19) Davis, S. M.; Gordon, B. E.; Press, M.; Somorjai, G. A. *J. Vac. Sci. Technol.* **1981**, *19* (2), 231.
(20) Davis, S. M.; Zaera, F.; Gordon, B. E.; Somorjai, G. A. *J. Catal.*, submitted for publication.
(21) Ibach, H.; Hopster, H.; Sexton, B. A. *Appl. Surf. Sci.* **1977**, *1*, 1.
(22) Malmstadt, H. V.; Enke, C. G.; Crouch, S. R. "Electronics and Instrumentation for Scientists"; The Benjamin/Cummings Publication Co., Inc.: Menlo Park, CA, 1981.
(23) Hubbard, A. T.; Anson, F. *Electroanal. Chem.* **1970**, *4*.
(24) Hubbard, A. T. *Crit. Rev. Anal. Chem.* **1973**, *3*, 201.
(25) Lai, C. N.; Hubbard, A. T. *Inorg. Chem.* **1972**, *11*, 2081.
(26) MacDonald, D. D. "Transient Techniques in Electrochemistry"; Plenum Press: New York, 1977.
(27) Collins, C. J.; Bowman, N. S. Eds. "Isotope Effects in Chemical Reactions"; Van Nostrand Reinhold Corp.: New York, 1970.
(28) Wieckowski, A. *J. Electroanal. Chem.* **1977**, *78*, 229.

Table II. Comparison of Ethylene Hydrogenation Kinetic Parameters for Different Platinum Catalysts

catalyst	log rate[a]	a^b	b^b	E_a, kcal/mol	ref
platinized foil	1.9	−0.8	1.3	10	46
platinum evaporated film	2.7	0	1.0	10.7	47
1% Pt/Al_2O_3		−0.5	1.2	9.9	48
platinum wire	0.6	−0.5	1.2	10	49
3% Pt/SiO_2	1.0			10.5	50
0.05% Pt/SiO_2	1.0	0		9.1	51
Pt(111)	1.4	−0.6	1.3	10.8	4
Pt(111)[c]				6	this work
Pt(polycrystalline)[d]	2.3	0	.75	5.9	this work

[a] Rate in (molecules/Pt surface atom)/s, corrected for the following conditions: T = 323 K, $P_{C_2H_4}$ = 20 torr, P_{H_2} = 100 torr. [b] Orders in ethylene (a) and hydrogen (b) partial pressure. [c] Temperature-programmed desorption of ethane from a Pt(111) surface first saturated with deuterium and then exposed to ethylene at 150 K (Figure 14). [d] Annealed polycrystalline Pt electrode; electroreduction at E = −0.200 V vs. AgCl/Ag with $[H^+]$ = 1 M.

Accordingly, L–S reduction of ethylene from the bulk solution must involve breaking or forming a specific C–H or Pt–H bond. The latter possibility, breakage of a Pt–H bond, seems more likely as discussed below.

It should be noted that ethylene electroreduction at Pt is zero order in ethylene concentration (pressure). Also, the dependence of the rate on electrode potential [as measured by the Tafel slope, $dE/d(\log \text{rate})$] is less than the 120-mV value expected for rate-determining electron-transfer reactions, implicating a reaction mechanism involving one or more reversible electron-transfer steps, followed by rate-determining chemical reactions.[29]

We now compare the rate law for L–S ethylene hydrogenation at polycrystalline Pt with that for G–S hydrogenation over Pt(111) single-crystal surfaces. Comparison of these G–S and L–S hydrogenations requires that the rate data not be mass-transfer limited. In the G–S reaction, the reaction rate (about 25 (molecules/Pt atom)/s) is orders of magnitude less than the molecular flux at the surface (about 10^6 (molecules/Pt atom)/s). Likewise, under L–S conditions, the initial rate (10^2 (molecules/Pt atom)/s) is much less than the collision rate. At potentials approaching the onset of hydrogen evolution, the limiting influence of diffusional transport was avoided by stirring the solution. The Pt(111) surface, as shown in Table II, behaves catalytically like polycrystalline Pt catalysts.

The G–S hydrogenation rate law at atmospheric pressures over either a clean or ethylene-pretreated surface has been reported and has the form[4]

$$\text{rate} = 8 \times 10^8 P_{C_2H_4}^{-0.6} P_{H_2}^{1.3} \exp(-E_a/RT) \quad (1)$$

where the rate is in (molecules/Pt atom)/s and E_a = 10.8 0.1 kcal/mol.

For similar surfaces, the L–S hydrogenation rate law for the clean (H-covered surface, Figure 2D) is

$$\text{rate} = 8.6 \times 10^6 a_{H^+} \exp\{-[E_a + 1.5F(E - E_0)]/RT\} \quad (2)$$

where E_a = 5.9 ± 0.6 kcal/mol and E_0 is defined below (eq 3). Over an ethylene-pretreated surface (Figure 2C) the rate law for the initial rate is the same, but the activation energy has a larger value of 6.6 ± 0.6 kcal/mol.

To compare eq 1 and 2, the potential dependence in the L–S reaction must be converted to an equivalent H_2 pressure. For that purpose, the Nernst equation is used, since the H_2/H^+ equilibrium is rapid:

$$E = E_0 + (2.3RT/F) \log (a_{H^+}/P_{H_2}^{0.5}) \quad (3)$$

where E_0 is the standard potential of the hydrogen electrode (NHE) vs. AgCl/Ag reference (E_0 = −0.204 V at 323 K). Assuming that the rate of L–S hydrogenation of ethylene at constant temperature and pH is controlled by the availability of hydrogen at the solid–liquid interface, eq 2 and 3 can be combined, with a_{H^+} = 1, to give

$$\text{rate} = 8.6 \times 10^6 P_{H_2}^{0.75} \exp(-E_a/RT) \quad (4)$$

Since the reaction rates are not mass-transfer limited, we conclude that the different rate laws (eq 1 vs. eq 4) for G–S and L–S hydrogenation of ethylene (especially the differing activation energies) indicate different reaction mechanisms. The mechanisms will be discussed in section 3.

2. Adsorbed Species. Having summarized and compared the macroscopic kinetic parameters, we now present and compare new and previous data on molecular aspects of the surface reaction in ethylene hydrogenation. In particular, we have characterized, before and after ethylene hydrogenations, the surfaces of single-crystal Pt catalysts using LEED, TPD, HREELS, AES, cyclic voltammetry, chronoamperometry, and a ^{14}C radiotracer technique. We present the results of these adsorbed species studies in three sections: (1) the structure of chemisorbed ethylene, (2) its reactivity with hydrogen, and (3) its reactivity with ethylene. In each section we present first the G–S data, then the L–S data, and finally a comparison of the two.

2.1. Structure of Chemisorbed Ethylene. 2.1a. Gas–Solid Conditions. Chemisorption studies in UHV (LEED,[30,31] UPS,[32] TPD,[33–35] and HREELS[33,36] have shown that ethylene adsorbs dissociatively on clean Pt(111) surfaces to form ethylidyne (CCH_3) at temperatures conducive to ethylene hydrogenation. In the conversion of ethylene to ethylidyne, a hydrogen atom from the ethylene bonds to the surface, recombines with another hydrogen atom, and desorbs as H_2. The remaining C_2H_3 fragment rearranges to form a methyl group which sits above the dehydrogenated carbon in a 3-fold hollow site on the Pt(111) surface. The activation energy for this UHV process is about 18 kcal/mol.[35]

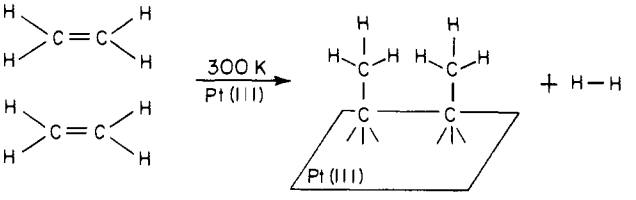

These ethylidyne (CCH_3) moieties also form on clean Pt(111) surfaces during ethylene hydrogenation at atmospheric pressures. Three separate techniques support this fact—TPD, LEED, and HREELS. The results of these three techniques for a Pt(111) surface after ethylene hydrogenation are compared with the "fingerprint" results for ethylidyne in Figure 3. The LEED pattern of the Pt(111) surface [a (2 × 2)] and the temperatures of hydrogen desorption in TPD from adsorbate decomposition after ethylene hydrogenation, as discussed previously,[4] both match those for ethylidyne on this surface.[30–33] The diffuseness of the $^1/_2$-order spots in LEED and the shaded shoulder in the TPD are probably due to minority C_xH_y fragments on the surface. HREEL vibrational spectra of the Pt(111) surface after ethylene hydrogenation, as shown in Figure 3, show peaks mostly attributable to ethylidyne, confirming the monolayer structure. C_xH_y species are again the most probable reason for the extra features. There is also a small amount of coadsorbed carbon monoxide. Finally,

(29) Vetter, K. J. "Electrochemical Kinetics, Theoretical and Experimental Aspects"; Academic Press: New York, 1967.

(30) Kesmodel, L. L.; Dubois, L. H.; Somorjai, G. A. *Chem. Phys. Lett.* **1978**, *56*, 267.
(31) Kesmodel, L. L.; Dubois, L. H.; Somorjai, G. A. *J. Chem. Phys.* **1979**, *70*, 2180.
(32) Albert, M. R.; Sheddon, L. G.; Eberhardt, W.; Greuter, F.; Gustafsson, T.; Plummer, E. W. *Surf. Sci.* **1982**, *120*, 19.
(33) Steininger, H.; Ibach, H.; Lehwald, S. *Surf. Sci.* **1982**, *117*, 685.
(34) Demuth, J. E. *Surf. Sci.* **1979**, *80*, 367.
(35) Salmeron, M.; Somorjai, G. A. *J. Phys. Chem.* **1982**, *86*, 341.
(36) Skinner, P.; Howard, M. W.; Oxton, I. A.; Kettle, S. F. A.; Powell, D. B.; Sheppard, N. *J. Chem. Soc., Faraday Trans. 2* **1981**, *77*, 1203. (a) Beeck, O. *Discuss. Faraday Soc.* **1950**, *8*, 118.

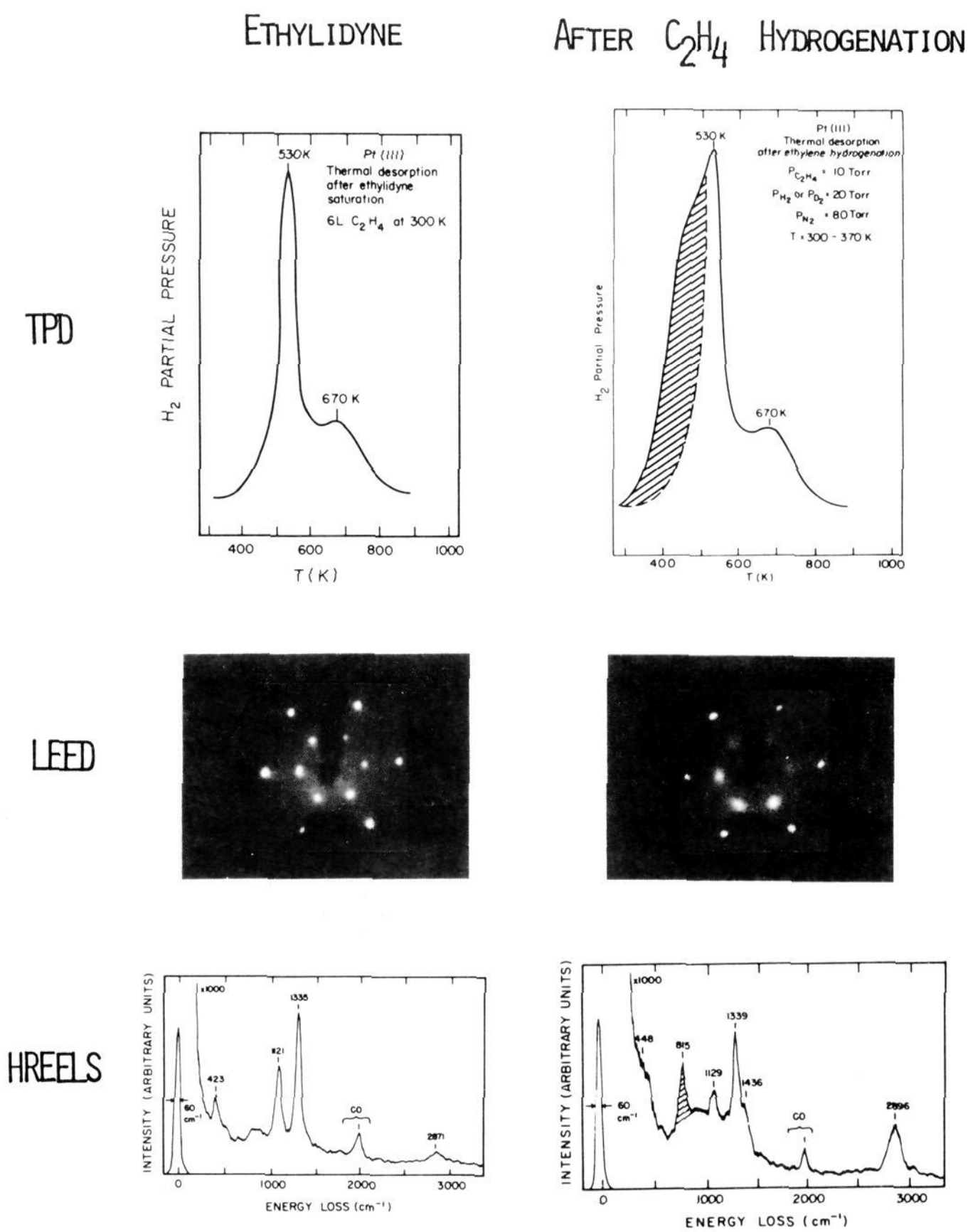

Figure 3. Evidence for the presence of ethylidyne on the Pt(111) surface after hydrogenation of gas-phase ethylene at atmospheric pressures over this surface. Temperature-programmed desorption, low-energy electron diffraction, and high-resolution electron energy loss spectroscopy data for ethylidyne are compared with the results of these techniques on Pt(111) after ethylene hydrogenation at atmospheric pressure and return of the crystal to vacuum.

hydrogenation reactions begun over either initially clean or ethylidyne-saturated Pt(111) surfaces prepared in UHV have identical rates.[4] Consequently, we conclude that ethylene chemisorbed as ethylidyne is present on the Pt(111) surface during G–S ethylene hydrogenation at atmospheric pressures. These results are in agreement with the pioneering catalytic work of O. Beeck in which he showed that preadsorption of ethylene on Pt films decreased the rate of ethylene hydrogenation by only 5%.[36a]

2.1b. Liquid–Solid Conditions. In the present work, LEED observations were made in UHV on ethylene adsorbed under L–S conditions. Such experiments were preceeded, as usual, by blank runs to determine whether accidental contamination of the surface occurred during transfer between vacuum and solution;[16,17] Auger spectra following the blank runs indicated a trace of carbon, $\Theta_C < 0.03$, presumably due to residual ethylene, and no change in the Pt(111) (1 × 1) LEED pattern. In contrast to the G–S result which produced a (2 × 2) LEED pattern,[4] adsorption of ethylene from solution at open circuit (rest potential about 0.02 V vs. Ag/AgCl) produced a (1 × 1) LEED pattern with noticable diffuse scattering.

On the basis of integration of Auger spectra of this surface, Figure 4, the carbon packing density (Θ_C) was about 1.5 times the packing density for saturation ethylidyne coverages. However, *determination of Θ_C in vacuum clearly underestimates the amount* of ethylene present when the Pt surface was in contact with solution: the anodic charge for electrochemical oxidation of the adsorbed ethylene decreased by 23% when the Pt surface was subjected to vacuum (as in Auger spectroscopy) prior to electrolysis in ethylene-free electrolyte, as discussed below. Adding this fraction to the amount observed by Auger spectroscopy places the packing density at saturation in L–S conditions at $\Theta_{C_{L\text{-}S}} \approx 2\Theta_{C_{G\text{-}S}}$.

We have investigated the structure of L–S adsorbed ethylene to compare with CCH_3. Auger spectra indicated that the nature of the adsorbed species formed under L–S conditions varies with electrode potential. Adsorption of C_2H_4 at potentials between 0 and 0.3 V (vs. AgCl/Ag) yielded surfaces relatively free of oxygenous species as judged from the Auger spectra, as seen for instance in Figure 4C. However, when adsorption was carried out either under more reducing ($E < 0$ V) or more oxidizing ($E > 0.3$ V) conditions, oxygen Auger signals appeared (510 eV,

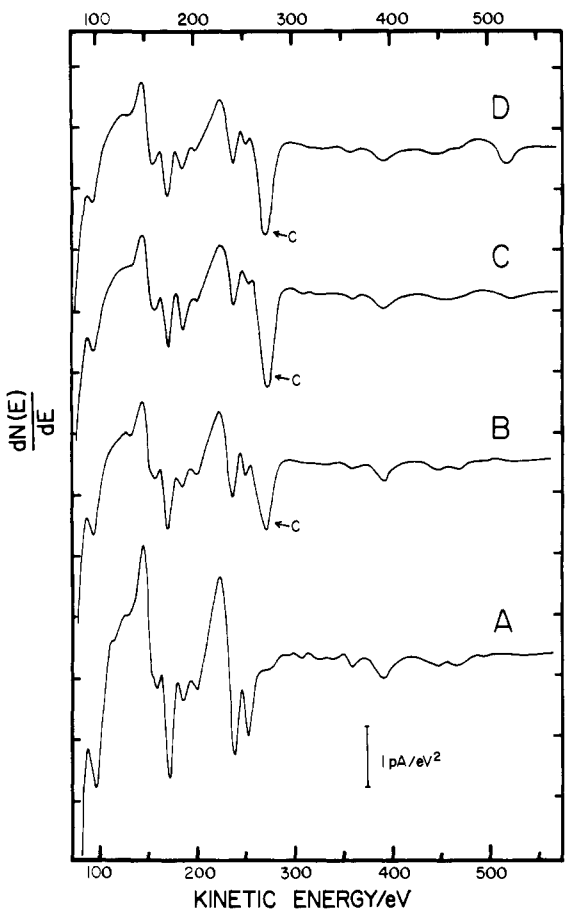

Figure 4. Auger electron spectra: (A) Pt(111) clean surface; (B) Pt-(111)(2 × 2)-C_2H_3; (C) Pt(111)(1 × 1)-C_2H_4, after L-S adsorption at open circuit (0.02 V); (D) Pt(111)(1 × 1)-C_2H_4 and oxygen-containing species adsorbed during a negative scan below 0 V. Experimental conditions: primary beam, 0.5 μA at 2,000 eV, angle of incidence, α_i = 73°, modulation amplitude (CMA), 5.00 V.

Figure 4D). Under oxidizing conditions, the oxygen signal results simply from the onset of oxidation of the Pt surface,[18,37] but the presence of oxygen signals under reducing conditions is surprising. A clue as to the origin of this oxygen signal was provided by the electrochemical data for this adsorbed layer: linear scan voltammograms for a smooth polycrystalline thin-layer electrode[38,39] in ethylene-free 1 M $HClO_4$ after treatment with ethylene solution at midrange (E = 0.2 V), Figure 5A, and reducing potentials (E = −0.1 and −0.2 V), Figure 5B,C, show the emergence of an oxidizable species (peak potential 0.5 V) under reducing adsorption conditions. While the identity of this species is unknown, it undergoes oxidation at potentials where species adsorbed from aqueous alcohol solutions react.[40] Voltammograms obtained for progressively more positive adsorption potentials, Figure 5D,E, illustrate the full course of this transition in reactive behavior.

It is interesting that disorder introduced into the Pt(111) surface by electrochemical oxidation[18,41] substantially altered the electrochemical behavior of adsorbed ethylene, particularly oxidation. These differences are illustrated by the voltammetric curves in Figure 6C,D.

Besides changes in the structure of L-S adsorbed ethylene with potential, there are also changes in coverage. Figure 7 shows the

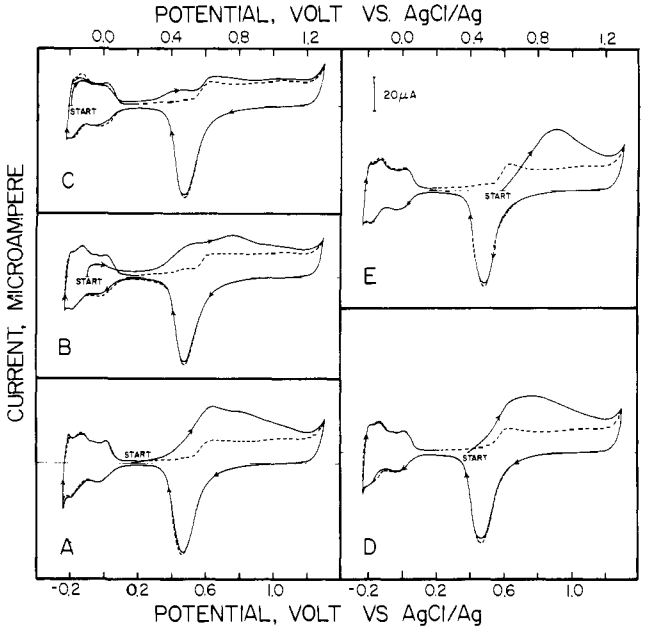

Figure 5. Cyclic current potential curves of polycrystalline Pt (TLE, ref 38, 39) electrode. L-S ethylene adsorbed: (A) at any potential between 0 and 0.3 V; (B) at −0.100 V; (C) at −0.200 V; (D) at +0.400 V; (E) at +0.600 V. (---) clean Pt surface, (—) Pt-C_2H_4 surface. Following ethylene adsorption, the TLE cavity was rinsed with 1 M $HClO_4$. Experimental conditions: adsorption time = 2 min; scan rate = 10 mV/s.

dependence of the charge involved in the oxidation of the L-S ethylenic moieties as a function of the electrode potential during adsorption. Provided that surface coverage is proportional to Q_{ox}, this plot represents the potential dependence of the surface coverage of the adsorbed organic material. As expected, ethylene packing density displays a maximum at potentials (0–0.2 V) intermediate between oxidation and reduction of adsorbed ethylene.

2.1c. Comparison of Gas-Solid and Liquid-Solid Conditions. The structure of L-S adsorbed ethylene within this potential window between oxidation and reduction of ethylene (0–0.2 V) is the most appropriate structure to compare to the ethylidyne structure of G-S adsorbed C_2H_4. Comparison of Auger spectra, Figure 4B,C, illustrates the consistent difference in carbon peak morphology for G-S and L-S adsorbed ethylene. The G-S carbon peak exhibits a hump on the low-energy side and is broader than the L-S carbon peak. This spectral difference, together with the integrated Auger electron spectra showing that L-S adsorbed ethylene was twice as densely packed on the Pt surface as ethylidyne, suggests a structural difference in L-S and G-S chemisorbed ethylene. To confirm that the G-S and L-S chemisorbed ethylene structures are different and to see if either is a hydrogenation reaction intermediate, we investigated the reactivity of G-S and L-S adsorbed ethylene with hydrogen and ethylene.

2.2. Reaction with Hydrogen. 2.2a. Gas-Solid Conditions. Reaction of G-S chemisorbed ethylene (ethylidyne) with H_2(g) was studied previously by a ^{14}C radiotracter technique[20] and here by high-resolution electron energy loss spectroscopy. In both experiments a saturation coverage of CCH_3 remains close to one monolayer coverage ($\theta/\theta_0 \approx 1$) at near room temperature. It was found in the previous ^{14}C experiments that only at temperatures above 330 K are the $^{14}C^{14}CH_3$ fragments appreciably hydrogenated and removed from the surface. Complementary HREEL spectra in Figure 8 prove that not only does this carbon remain on the surface, but the structure of this strongly adsorbed ethylidyne is the same before and after 1 atm of H_2 treatments, since these spectra are virtually identical. The increase in the CO (ν_{CO}) band intensity is the result of CO adsorption from background gases when a small fraction of the CCH_3 is hydrogenated and removed from the surface, but since CO has a large cross section for vibrational excitation, this increased peak intensity corresponds to less than 15% of a monolayer of chemisorbed CO.

(37) Angertein-Kozlowska, H.; Conway, B. E.; Sharp, B. A. *J. Electroanal. Chem.* **1973**, *43*, 9 (1973).
(38) Soriaga, M. P.; Hubbard, A. T. *J. Am. Chem. Soc.* **1982**, *104*, 3937.
(39) Soriaga, M. P.; Wilson, P. H.; Hubbard, A. T.; Benton, C. S. *J. Electroanal. Chem.* **1982**, *142*, 317.
(40) Stickney, J. L.; Soriaga, M. P.; Hubbard, A. T.; Anderson, S. E. *J. Electroanal. Chem.* **1981**, *125*, 73.
(41) Wieckowski, A.; Schardt, G. C.; Rosasco, S. D.; Stickney, J. L. Hubbard, A. T. *Surf. Sci.*, in press.
(42) Godbey, D.; Zaera, F.; Yeates, R.; Somorjai, G. A. *Surf. Sci.*, in press.

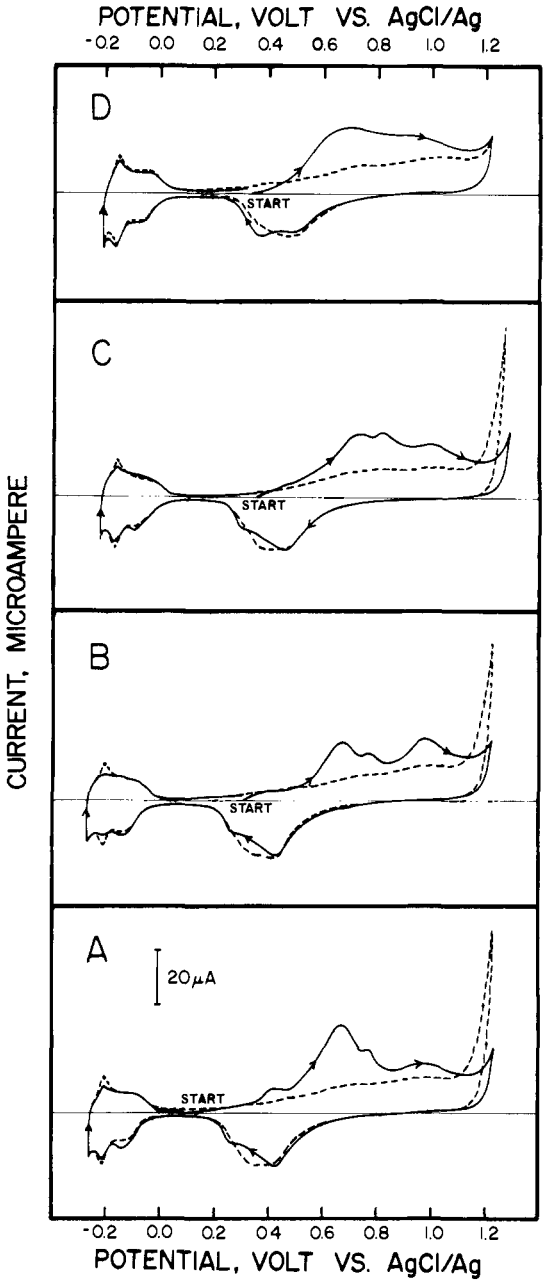

Figure 6. Cyclic current–potential curves of Pt(111) electrode obtained in 1 M $HClO_4$ electrolyte following (A) L–S adsorption of ethylene during negative scan (Figure 5A), (B) vacuum exposure of L–S ethylene adsorbed during the negative scan, (C) L–S adsorption of ethylene on Pt(111) at 0.35 V, (D) L–S adsorption of ethylene at 0.35 V on Pt(111) disordered by electrochemical oxidation. Scan rate = 10 mV/s.

We estimate the rate of ethylidyne rehydrogenation to be 10^{-4} (molecules/Pt atom)/s (Table III), over 4 orders of magnitude slower than the rate of ethylene hydrogenation at the same temperature and H_2 pressure.

2.2b. Liquid–Solid Conditions. Reaction of L–S chemisorbed C_2H_4 with H_2(g) was studied by cyclic voltammetry and by monitoring the coverage as measured by Q_{ox}. In contrast to the stability of G–S adsorbed ethylidyne to 1 atm of H_2 at 300 K, the L–S adsorbed species reacted with H_2 dissolved in aqueous electrolyte at atm of external pressure, both at open circuit and when the electrode potential was held at 0.200 V (Figure 9A). The reaction led to partial desorption (Table III), as well as to a change in chemical properties of the adsorbate, as evidenced by emergence of a new oxidative voltammetric peak near 0.5 V, Figure 9A as compared with Figure 5A; the size of this new peak increased with increasing exposure to H_2, Figure 9B,C. The surface species produced by this transformation have not been

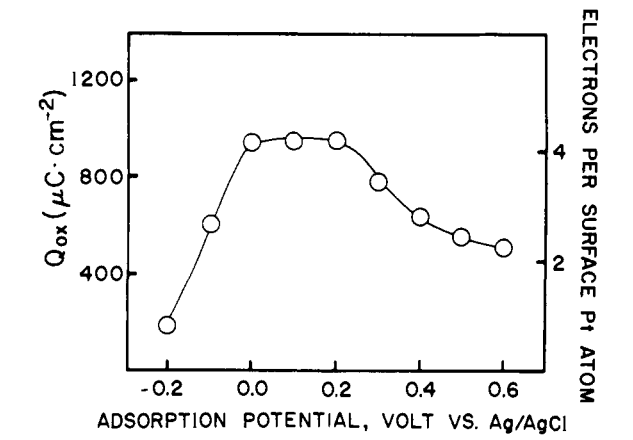

Figure 7. Anodic charge for L–S oxidation of adsorbed ethylene and number of electrons per surface Pt atom, as a function of adsorption potential.

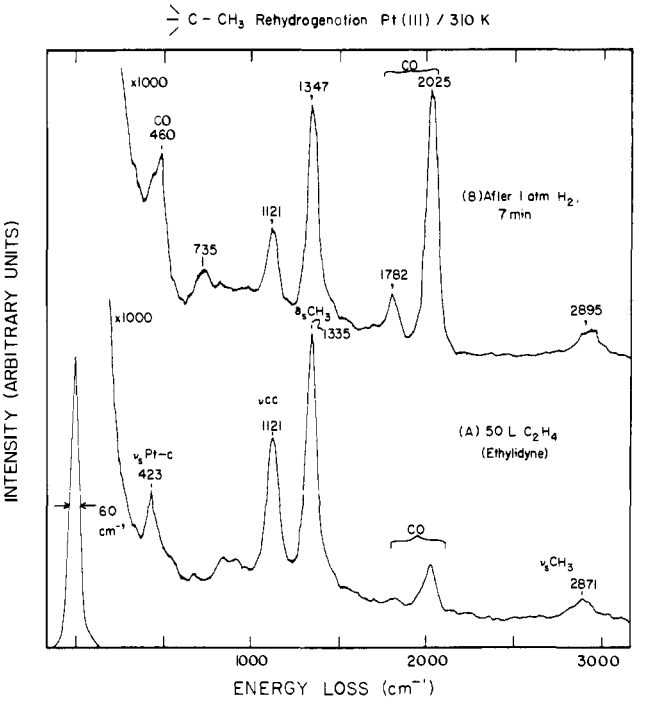

Figure 8. Stability of ethylidyne species on Pt(111) under 1 atm of H_2(g). HREEL vibrational spectrum of ethylidyne (a) before and (b) after 1 atm of H_2 for 5 min at 310 K.

identified, although the oxidative voltammetric peak is suggestive of adsorbed alcohols[40] and the Auger spectra display an oxygen signal, Figure 4D.

2.2c. Comparison of G–S and L–S Conditions. The lack of reactivity of G–S adsorbed ethylene with H_2 as compared with L–S adsorbed ethylene reactivity is not due to a blocking of sites for H_2 adsorption as shown by temperature-programmed desorption. Figure 10 shows TPD results for coadsorption of $H_2(D_2)$ on an ethylidyne-saturated surface (coverage typical for ethylene hydrogenation). H(D) atoms coadsorbed on the Pt surface desorb as $H_2(D_2)$ at below 300 K, while CCH_3 decomposes to evolve H_2 at >500 K. While very little coadsorption was possible with low-pressure exposures of H_2 (less than 10^{-5} torr), coadsorption of $H_2(D_2)$ was possible with 1-atm exposures of these gases as shown by the presence of the 300 K desorption peak in Figure 10.

Furthermore, while the reaction of ethylidyne with H_2(g) showed none of the irreversible structure changes seen for L–S chemisorbed $C_2H_4 + H_2$, there were reversible structure changes as evidenced by reactions with D_2. HREELS studies (not shown here) of the ethylidyne reaction with 1 atm of deuterium show

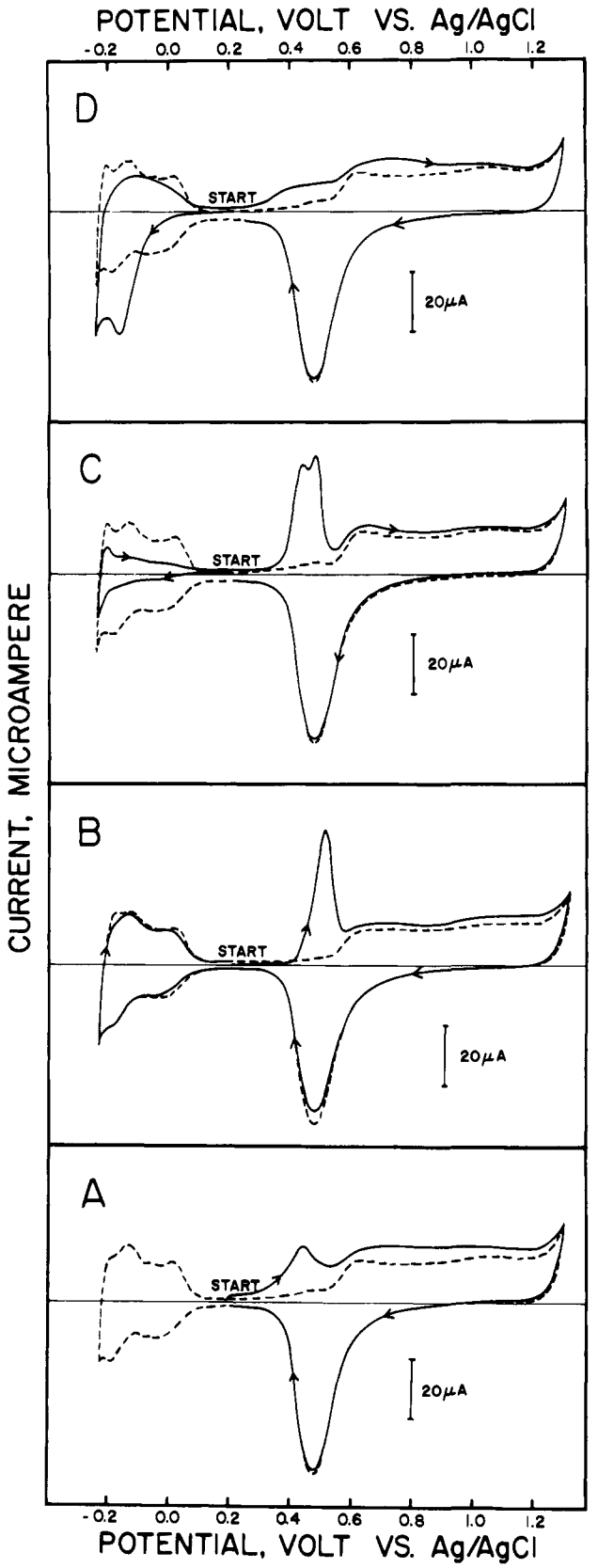

Figure 9. Cyclic current–potential curves for L–S adsorbed ethylene at polycrystalline Pt(TLE) electrodes. Ethylene adsorption at 0.2 V was followed by (A) rinsing the C_2H_4 coated electrode with H_2-saturated electrolyte at 0.2 V, (B and C) gaseous hydrogen at 1 atm and (D) negative-going potential scan (without hydrogenation). Scan rate = 10 mV/s.

that there is a small amount of H–D exchange in the methyl group. Similar HREELS results for H,D exchange in CCH_3 on Rh(111) have been reported and a mechanism has been proposed.[43] Again,

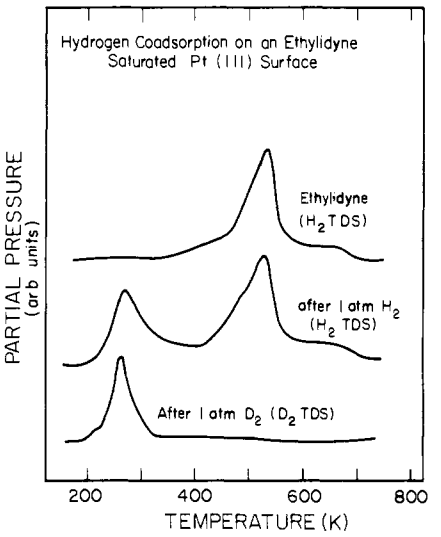

Figure 10. Temperature-programmed desorption to show coadsorption of hydrogen with a monolayer of ethylidyne (CCH_3) on Pt(111) by 1-atm exposure of H_2. (A) Saturation coverage of CCH_3/TPD amu = 2; (B) saturation coverage of CCH_3 + 1 atm of H_2/TPD amu = 2; (C) saturation coverage of CCH_3 + 1 atm of D_2/TPD amu = 4. The desorption peak near 300 K corresponds to $H_2(D_2)$ desorbing from the bare Pt(111) surface. The higher temperature H_2 desorption results from the decomposition of CCH_3 to give H_2 and surface carbon.

the rate of this process on Pt(111) is estimated to be less than 10^{-5} molecules/Pt atom)/s, orders of magnitude slower than ethylene hydrogenation (Table III).

G–S and L–S adsorbed C_2H_4 also react differently with electrogenerated hydrogen as shown by the linear scan voltammetric data in Figure 11. The ethylidyne species characteristic of G–S adsorption is much less reactive electrochemically, Figure 11A, than the L–S adsorbed species, Figure 11B, toward both reduction (dotted curves) and oxidation (solid curves). The lower reactivity of G–S adsorbed ethylene (ethylidyne) toward electrogenerated H atoms correlates with the slow rehydrogenation rate of CCH_3 under 1 atm of gas-phase H_2 (section 2.1a).

By comparing the rates of reaction of G–S and L–S chemisorbed C_2H_4 with $H_2(D_2)$ to the ethylene hydrogenation rates under similar conditions (Table III), we conclude that ethylene chemisorbed under G–S conditions as ethylidyne is too stable to be a hydrogenation intermediate at 300 K, but L–S chemisorbed C_2H_4 is a possible intermediate in the L–S hydrogenation.

2.3. Reaction with C_2H_4. 2.3a. Gas–Solid Conditions. It has already been noted (section 2.2a) that the ethylidyne (present on Pt(111) surfaces during the G–S hydrogenation of C_2H_4) is not a reaction intermediate. HREELS studies also show that C_2H_4 cannot be irreversibly adsorbed in an ethylidyne monolayer, even at 1 atm of pressure. HREEL studies in Figure 12 show the fingerprint spectra of CCD_3 (A), CCH_3 (C), and a CCD_3 monolayer exposed to 1 atm of C_2H_4 (B). This latter spectrum shows no sign of the intense δ_s CH_3 mode (1340 cm^{-1}) for CCH_3. This mode would appear if there were C_2H_4 coadsorption or replacement of CCD_3 to form CCH_3. There is also no evidence for a CH_2 scissor vibration (1400–1500 cm^{-1}) for associatively adsorbed ethylene.

2.3b. Liquid–Solid Conditions. Despite their lower electrochemical reactivity, ethylidyne-covered Pt(111) surfaces prepared in UHV-catalyzed electrochemical reduction and oxidation of ethylene from solution identically with the clean Pt(111) surface (Figure 13). This surprising result is rendered more understandable by the observation that exposure of the ethylidyne layer to aqueous ethylene solution at open circuit converted the ethylidyne to a form apparently identical with the L–S adsorbed species as evidenced by the identical appearance of the LEED patterns [(1×1) with noticeable diffuse intensity], identical Auger spectral morphology, Figure 4C, and identical electrochemical behavior,

(43) Koel, B. E.; Bent, B. E.; Somorjai, G. A. *Surf. Sci.* **1984**, *146*, 211.

Table III. Rates of Hydrogen-Transfer Processes at T = 323 K on Pt(111) and Annealed Polycrystalline Pt Electrode Surfaces

surface	process	conditions	est turnover rate, (reactions/ Pt atom)/s	ref
Pt(111)	C_2H_4 hydrogenation	$P_{C_2H_4}$ = 20, P_{H_2} = 100 torr	25	*a*
Pt(polycrystalline)	C_2H_4 electroreduction from solution	$P_{C_2H_4}$ = 20,[f] P_{H_2} = 100 torr	187	*b*
Pt(111)	hydrogenation and removal of G–S chemisorbed ethylene from the surface by H_2(g)	P_{H_2} = 760 torr, $\theta_{C_2H_4}$ = satn	10^{-4}	*c*
Pt(polycrystalline)	hydrogenation and removal of L–S chemisorbed ethylene from the surface by H_2(g)	P_{H_2} = 760 torr, $\theta_{C_2H_4}$ = satn	>0.1	*d*
Pt(polycrystalline)	hydrogenation and removal of L–S chemisorbed ethylene from the surface by electrogenerated H atoms	[H^+] = 1 M, E = −0.176 V, $\theta_{C_2H_4}$ = satn	2.2	*b*
Pt(111)	H,D exchange in the methyl group of ethylidyne using D_2(g)	$\theta_{C_2H_4}$ = satn, P_{D_2} = 1 atm	10^{-5}	*e*

[a] Reference 4. [b] This work. [c] ^{14}C radiotracer studies—this work and ref 21. [d] Extent of reaction monitored by total oxidation charge which is compared to O_{ox} in Figure 12. [e] Estimated from HREELS data mentioned here and to be discussed more fully later. Similar data have been discussed for Rh(III), ref 4. [f] The reaction was run in solution with [H^+] = 1. The effect of potential has been converted to an effective H_2 pressure by using eq 2–4.

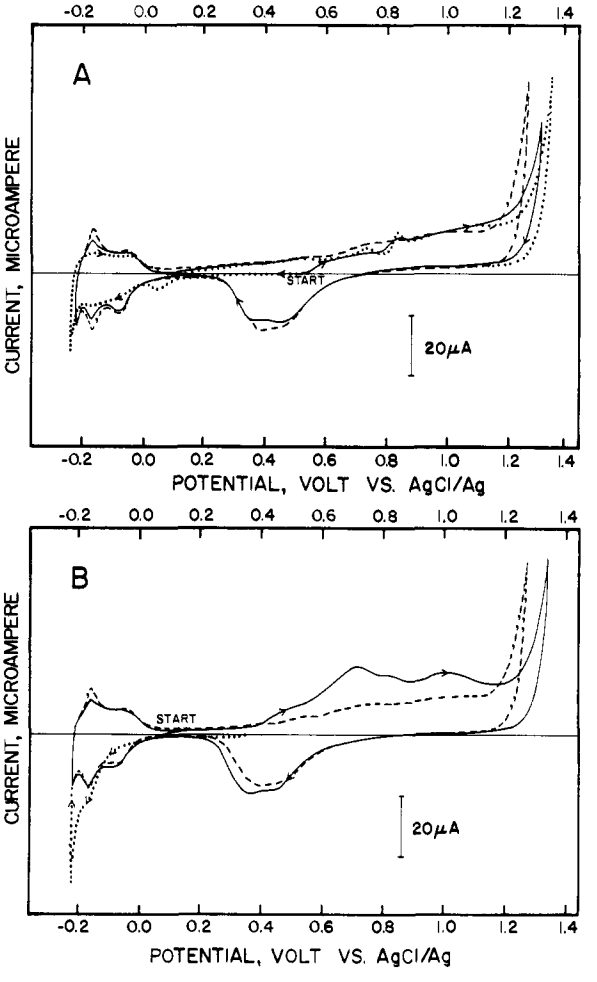

Figure 11. Cyclic current–potential curves of Pt(111) electrode. (A) Following G–S adsorption of ethylidyne: (—) positive going scan starting from rest potential (0.6 V), (•••) negative going scan, and (---) subsequent cyclic scan characteristic of the "disordered" Pt(111) surface. (B) Following L–S adsorption of ethylene at open circuit (0.20 V) and rinsing with pure electrolyte. Scan rate = 10 mV/s.

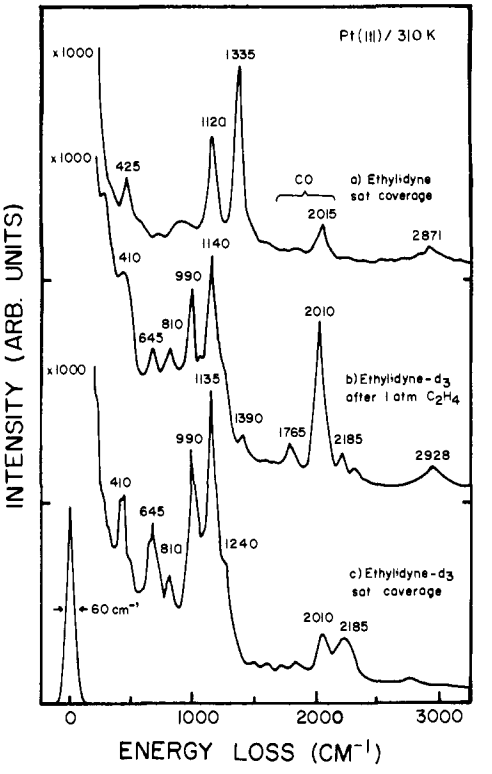

Figure 12. High-resolution electron energy loss vibrational spectra to show that ethylene cannot be irreversibly coadsorbed in an ethylidyne monolayer even under atmospheric pressure exposures. (A) Ethylidyne, CCH_3; (B) ethylidyne-d_3 + 1 atm of C_2H_4 for 5 min; (C) ethylidyne-d_3.

Figure 11B. That this interconversion is due to displacement of adsorbed ethylidyne by ethylene rather than to a reduction process of ethylidyne is indicated by the fact that interconversion does not occur in the absence of dissolved ethylene; voltammetric behavior identical with Figure 11A was still obtained, and the LEED pattern was still (2 × 2) although sharpened somewhat. In other words, exposure of the ethylidyne-coated surface to aqueous ethylene in the appropriate potential window (0–0.2 V) regenerates the reactive ethylene intermediate by replacement. By contrast, as noted earlier, G–S ethylidyne reacted extremely slowly with molecular C_2H_4 in the gas phase (Figure 12).

2.3c. Comparison of G–S and L–S Conditions. While G–S adsorbed ethylidyne can be converted to the L–S adsorbed form in solution, the reverse is not true. Exposure of L–S adsorbed ethylene to vacuum or ethylene vapor altered the behavior of the adsorbed layer somewhat, but did not produce adsorbed ethylidyne, as evidence by voltammetric scans following vacuum treatment, Figure 6B: smaller oxidative charges resulted for samples that had been evacuated, although the locations of the peaks were the same. Comparison of Figure 11A with Figure 6B, for adsorbed ethylidyne, illustrates this vastly different behavior.

2.4. Summary of G–S and L–S Chemisorbed Ethylene Structure and Reactivity. In comparing the adsorbed ethylene species that cover these Pt surfaces during ethylene hydrogenation, we conclude from the preceeding data that (1) chemisorbed ethylene structures are different for G–S and L–S reactions (the gas phase structure is ethylidyne (CCH_3) and the L–S product is, most probably, densely packed, undissociated ethylene), (2) the G–S formed structure is stable in vacuum and does not react with C_2H_4(g) (it can be converted to L–S chemisorbed ethylene on exposure to aqueous ethylene at open circuit), (3) the L–S formed structure

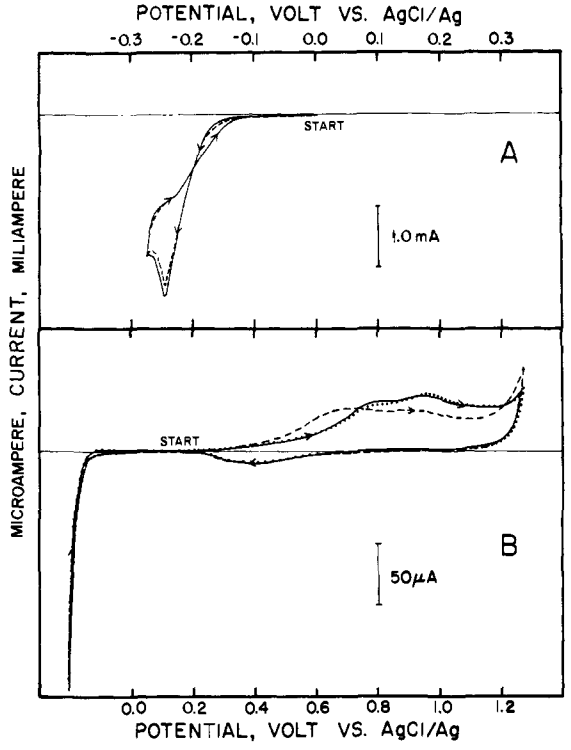

Figure 13. Cyclic current–potential curves of (—) initially clean Pt(111) electrode and (---) Pt(111)–C_2H_3 surface, recorded in 1 M $HClO_4$ saturated with ethylene. (A) Negative going scan; (B) positive going scan: (•••) subsequent cyclic scan characteristic of the disordered Pt(111) surface. Scan rate = 10 mV/s.

is stable in vacuum and more reactive electrochemically in acidic solution than the G–S structure (it does not convert to CCH_3 when transferred to vacuum, (4) the G–S adsorbate is inert toward molecular hydrogen (although H_2 can be adsorbed and dissociated on the surface), while the L–S material reacts actively with H_2 in the aqueous environment, (5) at potentials approaching the onset of hydrogen evolution, chemisorbed ethylene is reductively desorbed from the surface and partially converted to alcohol-related chemisorbed products, (6) G–S adsorbed ethylene is irreversibly adsorbed and is not a hydrogenation reaction intermediate at 300 K, and (7) G–S and L–S adsorbates can be characterized in vacuum without altering their catalytic or electrochemical activity and with only partial desorption of the adsorbate.

3. Modeling the L–S Hydrogenation in G–S UHV Experiments. Since ethylene cannot be adsorbed on the catalytically active Pt(111) surfaces that are "saturated" with CCH_3 during C_2H_4 hydrogenation at 300 K, the steady-state hydrogenation of ethylene at the G–S interface at this temperature (if a minority of "defect sites" are not the catalyst) occurs on top of this layer of ethylidyne. By contrast, the L–S hydrogenation of C_2H_4 may occur directly on a H-covered Pt surface since L–S chemisorbed ethylene can be hydrogenated and removed from the surface at 300 K. The possibility that the L–S hydrogenation occurs on the surface and the G–S hydrogenation in a second layer above the surface could explain the higher activation energy for the G–S reaction (10.8 as compared to 5.9 kcal/mol) and suggests that ethylidyne inhibits the G–S reaction.

To test this hypothesis, we have modeled the proposed mechanism of L–S hydrogenation on the Pt surface in ultrahigh vacuum using temperature-programmed desorption. Thermal decomposition of ethylene over a Pt(111) surface results in the desorption of some ethane, product of self-hydrogenation (Figure 14, dashed-line spectra). The limiting step for this process is the decomposition of ethylene which provides surface hydrogen atoms for the hydrogenation.[42] When the surface is predosed with H_2 followed by ethylene, the ethane thermal desorption peak broadens and shifts to lower temperatures (Figure 14, solid line). Using the method of Chan and Weinberg,[44] we obtain that the activation

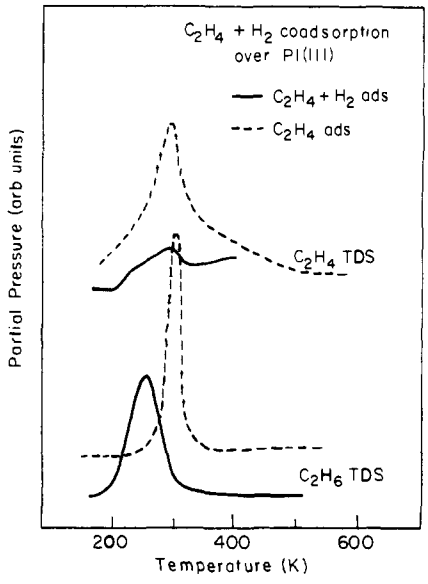

Figure 14. C_2H_4 (27 amu) and C_2H_6 (30 amu) TDS curves for C_2H_4 adsorbed over clean (dashed lines) and hydrogen predosed (solid lines) Pt(111) surfaces at 150 K. Exposures were 6 L for C_2H_4 and 30 L for hydrogen. Peak widths and maxima are used to calculate activation energies for the hydrogenations (see text).

energy of ethane production changes from 18 kcal/mol for the self-hydrogenation to 6 ± 1 kcal/mol when hydrogen is preadsorbed. Furthermore, if D_2 is used instead of H_2, deuterated ethane is produced. The activation energy for hydrogenation of ethylene with preadsorbed H_2 is, within experimental error, the same as was found for L–S ethylene hydrogenation, supporting the hypothesis that the L–S hydrogenation occurs on the Pt surface.

4. G–S and L–S Ethylene Hydrogenation Mechanisms. On the basis of the observations described in the text and summarized in Tables I–III, the following mechanism for the steady-state G–S hydrogenation of ethylene at 300 K is proposed (Figure 15A and ref 4):

$$D_2(g) \rightarrow 2D(ads) \quad (5)$$

$$2Pt_3\text{–}CCH_3 + 2D(ads) \rightarrow 2Pt_n\text{–}CDCH_3 \quad (6)$$

$$2Pt_n\text{–}CDCH_3 + C_2H_4(\text{weakly ads}) \rightarrow 2Pt_3\text{–}CCH_3 + C_2H_4D_2(g) \quad (7)$$

The presence of ethylidene species ($CHCH_3$) that form reversibly under high pressures of H_2 has been suggested previously.[4,35,43] This mechanism explains how hydrogen atoms adsorbed on the surface are transferred to ethylene on top of an irreversibly adsorbed layer of ethylidyne. The addition of the hydrogen atoms to ethylene in a second layer is probably sequential (rather than concerted) as previously shown for other metals.[2] The major difference between this mechanism and most previously proposed ones is that the hydrogenation occurs in a second layer above the catalyst. The idea of an adsorbed hydrocarbon being the source of hydrogen for hydrogenations was first proposed by Thomson and Webb[3] to explain much of the literature G–S C_2H_4 hydrogenation data. The similarity between reduction rate data for single-crystal and supported Pt surfaces noted earlier can be attributed to masking of the surface structure by the carbonaceous (CCH_3) deposit.[4]

According to the L–S results (Tables I and III), the following mechanism is proposed for the steady-state electroreduction of ethylene to ethane at 300 K (Figure 15B):

$$2D^+ + 2e^- \rightleftarrows 2D(ads) \quad (8)$$

$$D(ads) + C_2H_4(aq) \rightleftarrows Pt\text{–}C_2H_4D \quad (9)$$

$$Pt\text{–}C_2H_4D + D(ads) \xrightarrow{rds} C_2H_4D_2(aq) \quad (10)$$

(44) Chan, C. M.; Weinberg, W. H. *Appl. Surf. Sci.* **1978**, *1*, 377.

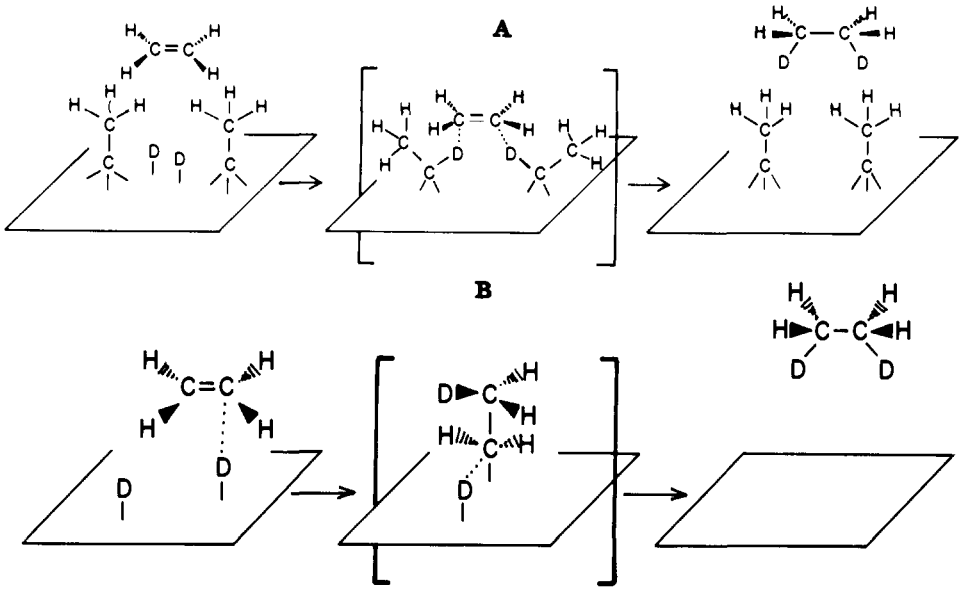

Figure 15. Proposed mechanisms for the steady-state hydrogenation of ethylene. (A) Gas-phase ethylene at atmospheric pressures over a Pt(111) surface at 300 K. (B) Ethylene in aqueous solution over a Pt surface at 300 K and −0.200 V. Other mechanisms are operative at higher temperatures and under non-steady-state conditions.

This mechanism is consistent with the observed dependence of the rate on potential (Tafel slope). As mentioned previously, the 40-mV Tafel slope for reduction of ethylene from bulk solution can be attributed to two reversible electrochemical reduction steps [(8) and (9)], followed by a rate-determining chemical reaction. The hypothesis that ethylene does not actually chemisorb on the surface as an intermediate in the L–S hydrogenation to ethane is supported by the fact that chemisorbed ethylene has a different activation energy and larger Tafel slope for reduction to ethane (Table I). This latter reaction is probably the result of an initial rate-determining electron transfer to chemisorbed ethylene followed by hydrogenation steps. It is noteworthy that eq 10 is identical with that first postulated by Horiuti and Polanyi[45] and confirmed recently by Kita.[8]

The primary reason for the activation energy difference in the G–S and L–S hydrogenations is that the interfering hydrocarbon layer is removed in the L–S reaction by electrochemical reduction of most of the chemisorbed ethylene. Owing to the absence of a blocking hydrocarbon layer, ethylene molecules can react directly with adsorbed hydrogen atoms in the L–S hydrogenation. The fact that the activation energy for L–S ethylene hydrogenation is the same as that determined by TPD for the reaction of gas-phase ethylene with adsorbed H atoms supports this conclusion.

In comparing the G–S and L–S ethylene hydrogenation mechanisms, we conclude (1) G–S reduction of ethylene occurs by hydrogen atom transfer from the Pt surface through a chemisorbed C_2H_3 (ethylidyne) layer to gas-phase C_2H_4 and (2) L–S reduction of ethylene occurs by reaction of ethylene with electrogenerated H atoms on the platinum surface.

Conclusions

The structures and reactivity of ethylene chemisorbed on platinum under G–S and L–S ethylene hydrogenation reaction conditions at 300 K are different. As a consequence, the hydrogenation processes occur via different pathways and are limited by different rate-determining steps. L–S reduction of ethylene proceeds by reaction with hydrogen atoms adsorbed on the platinum surface, while G–S hydrogenation of ethylene requires transfer of hydrogen atoms from the surface via irreversibly chemisorbed ethylene to weakly adsorbed ethylene in a second layer. The activation energies for these processes are 5.9 and 10.8 kcal/mol respectively. Temperature-programmed desorption experiments in ultrahigh vacuum support this lower activation energy for reduction of ethylene in direct contact with hydrogen on the surface.

Our results also show that the G–S and L–S adsorbates can be characterized in vacuum without loss of their catalytic or electrochemical activity and with only partial desorption of the adsorbate. The voltammetric behavior of L–S adsorbed ethylene is more clearly resolved on Pt(111) than on polycrystalline or disordered Pt surfaces.

Acknowledgment is made to the National Science Foundation, and the donors of the Petroleum Research Fund, administered by the American Chemical Society, for support of this research. The gas-phase reactions and adsorbate characterization were supported by the Director, Office of Energy Research, Office of Basic Energy Science, Materials Sciences Division of the U.S. Department of Energy under Contract DE-AC03-76SF00098. B.E.B. acknowledges the support of an NSF graduate fellowship.

Registry No. C_2H_4, 74-85-1; Pt, 7440-06-4.

(45) Horiuti, J.; Polanyi, M. *Trans. Faraday Soc.* **1934**, *30*, 1164.
(46) Farkas, A.; Farkas, L. *J. Am. Chem. Soc.* **1938**, *60*, 22.
(47) Beeck, O. *Rev. Modern Phys.* **1945**, *17*, 61.
(48) Bond, G. C. *Trans. Faraday Soc.* **1956**, *52*, 1235.
(49) Kazanskii, V. B.; Strunin, V. P. *Kinet. Catal.* **1960**, *1*, 517.
(50) Dorling, T. A.; Eastlake, M. J.; Moss, R. L. *J. Catal.* **1969**, *14*, 23.
(51) Schlatter, J. C.; Boudart, M. *J. Catal.* **1972**, *24*, 482.